Hindawi
International Transactions on Electrical Energy Systems
Volume 2023, Article ID 5514460, 9 pages
https://doi.org/10.1155/2023/5514460

Research Article

An Ultrashort-Term Wind Power Prediction Method Based on a Switching Output Mechanism

Rongqiang Feng,[1] Biheng Wang,[1] Xueqiong Wu,[1] Chenxi Huang,[1] Lei Zhao,[1] Wei Tang,[1] Kun Zhang,[1] Xiaoming Huang,[1] and Wei Ding[2]

[1]*NARI Group Corporation (State Grid Electric Power Research Institute), Nanjing, China*
[2]*Shandong Provincial Key Laboratory of Computer Networks, Shandong Computer Science Center (National Supercomputer Center in Jinan) Qilu University of Technology (Shandong Academy of Sciences), Jinan, China*

Correspondence should be addressed to Wei Ding; dingw@sdas.org

Received 30 January 2023; Revised 4 March 2023; Accepted 20 March 2023; Published 30 March 2023

Academic Editor: Xueqian Fu

The ultrashort-term wind power prediction (USTWPP) technology assists the grid to arrange spare capacity, which is important to optimize power investment reasonably. To improve the accuracy of USTWPP and optimize power investment requirements, a USTWPP method with dynamic switching of multiple models is proposed. For high wind speed fluctuation samples, the wind speed-power curve (WSPC) is fitted in a large sample of historical data, and the corrected wind speed is the input of WSPC. The spatiotemporal attentive network model (STAN) is built for the prediction of low wind speed fluctuation samples. According to the real-time fluctuation characteristics of the correction wind speed, a switching mechanism between multiple models is established to reconstruct the prediction results along the time axis direction, and the predicted power is set to zero for the samples whose correction wind speed is lower than the cut-in wind speed. We conducted simulation experiments with data provided by a wind farm with an installed capacity of 130.5 MW in China. The normalized root mean square error (NRMSE) for the 4 h ahead predicted power reaches 0.0907, which verified the validity and applicability of the proposed model.

1. Introduction

Wind energy is an important clean energy source, and according to the International Energy Agency [1], the total installed renewable energy capacity worldwide is expected to grow by 1200 GW between 2019 and 2024, with onshore wind accounting for a quarter of the growth [2, 3]. Affected by the randomness, volatility, and intermittency of wind power, wind power presents a high degree of uncertainty [4–6]. Large-scale wind power grid connection brings serious challenges to power system security. At this stage, accurate power forecasting is one of the key technologies to ensure the stable operation of power systems. According to the prediction time scale, wind power prediction (WPP) is divided into long-term prediction, medium-term prediction, short-term prediction, and ultrashort-term prediction [7–9].

The USTWPP outputs the power series in the next 4 h at the forecast moment with a resolution of 15 min, which provides technical support for scheduling departments to arrange spare capacity and unit control strategies [10]. According to the prediction strategy, it is divided into statistical learning methods and physical prediction methods [11, 12].

The physical prediction method needs to obtain the initial values and boundary conditions of the atmospheric operation and then solve the set of dynamical equations of the meteorological system to predict future meteorological data [13]. Then, the wind speed (WS) and wind direction

(WD) at the hub height are calculated according to the topography and geomorphology of the wind farm (WF), and the WSPC is further fitted to obtain the WPP model. The physical prediction method does not require a large amount of historical data accumulation but requires high computational resources and relies excessively on numerical weather prediction (NWP), which does not apply to the USTWPP business that requires high-frequency refreshing [14].

The statistical methods are the process of statistical inference of the external variation patterns of wind resources or wind power, where the external variation patterns (statistical properties) of wind power are analyzed and estimated from the samples of wind power data and inferred from its future development [14]. The statistical models apply the algorithms such as time series prediction [15], Kalman filtering [16], and support vector machine (SVM) [17], Khorramdel. With the rapid development of the application of deep learning techniques in power systems, recurrent neural networks and their variants, represented by long and short-term memory networks (LSTM), are widely used in the field of WPP.

In the current research on USTWPP, the hybrid model has higher prediction accuracy because of its adaptability to more specific scenarios. Shahid et al [18] proposed a prediction model of power sequence decomposition, independent modeling, swarm intelligent optimization parameters, and reconstruction of prediction results, which improved prediction accuracy by reducing efficiency. Wang et al [19] put forward the combined prediction model of error quadratic prediction and error correction, which can reduce the prediction error to a certain extent. In addition, there is a combinatorial prediction model with weighted combinations of multiple predictors such as the equal weight method [20], entropy method [21], and Bayesian method [22]. This kind of method has a high degree of refinement, but the weight setting is difficult to reach the optimal state, especially the time-varying weight is difficult to self-adapt. The current hybrid prediction models have achieved certain accuracy improvements and have been applied in certain engineering demonstrations. However, the current hybrid prediction models mostly adopt the mode of static combination, and there is less research on the combination mode of automatic coordination of different subprediction models.

To address the abovementioned problems, a USTWPP method based on a dynamic switching output mechanism is proposed, and the main contributions are as follows:

(i) A spatiotemporal attention neural network is developed in the course of training, and attention mechanisms are incorporated from both spatial and temporal channels, which improves the model's focus on key features. The proposed model is used to predict low WS fluctuation samples.

(ii) The LSTM model was used to correct the forecast WS, and the WS fluctuations in the forecast period were judged by the corrected WS. The samples with high fluctuations were predicted by fitting the WSPC. For samples where the corrected WS is lower than the cut-in WS of the wind turbine, the predicted power is set to 0.

(iii) A dynamic switching mechanism between the deep learning model and WSPC was established to improve the automation level of the WPP model. The validity of the proposed model is proved by the experimental analysis of the data provided by a wind farm with an installed capacity of 130.5 MW in China.

The rest of the paper is organized as follows: the second part is the theoretical modeling of the proposed method, the third part is the experimental analysis, and the fourth part is the conclusion of this paper.

2. The Ultrashort-Term Wind Power Prediction Methods

2.1. Modeling of WPP Based on Spatiotemporal Attention Neural Network. In the training process of LSTM in this paper, the attention mechanism is introduced in both temporal and spatio channels to enhance the attention to important features, so as to improve the modeling accuracy. Meanwhile, the introduction of the attention mechanism can improve the spatiotemporal interpretability of the model [23, 24].

Let the input data contain m spatial features, and for the input time step t, the attention weight vector of its spatial features is calculated as the following equation:

$$e_t = \sigma\left(W_e x_t + b_e\right), \tag{1}$$

where $\alpha_k^t = \exp\left(e_k^t\right)/\sum_{i=1}^m e_i^t$ represents the attention weight vector of each feature, W_e is the weight matrix, $\alpha_k^t = \exp\left(e_k^t\right)/\sum_{i=1}^m e_i^t$ represents the bias vector of the attention weight vector, $\sigma(g)$, and $\alpha_k^t = \exp\left(e_k^t\right)/\sum_{i=1}^m e_i^t$ represents the Sigmoid activation function.

The softmax function is used to normalize $\alpha_k^t = \exp\left(e_k^t\right)/\sum_{i=1}^m e_i^t$ and obtain the set of normalized attention weights for each feature $\alpha_k^t = \exp\left(e_k^t\right)/\sum_{i=1}^m e_i^t$. For the kth feature, $\alpha_k^t = \exp\left(e_k^t\right)/\sum_{i=1}^m e_i^t$, the attention weights are calculated as shown in the following equation:

$$\alpha_k^t = \frac{\exp\left(e_k^t\right)}{\sum_{i=1}^m e_i^t}. \tag{2}$$

The weighted feature vector j is obtained by superimposing the attention weight vector and the input feature vector j.

Let the input time-step be j and its temporal attention weight vector be calculated as shown in the following equation.

$$\beta_t = \mathrm{Re}LU\left(W_d h_t + b_d\right), \tag{3}$$

where $\beta_t = [\beta_1^t, \beta_2^t, \ldots, \beta_j^t]$, and W_d is the neural network weight matrix, b_d is the bias vector of temporal attention weights, and $\mathrm{ReLU}(\bullet)$ denotes the activation function.

The softmax function is used to normalize β_t, and the normalized attention weight $\varepsilon_t = [\varepsilon_1^t, \varepsilon_2^t, \ldots, \varepsilon_j^t]$ is obtained.

The attention weight of each moment and the state of hidden layer neurons were weighted to obtain the state of time sequence information h_t', as shown in the following equations.

$$\varepsilon_\tau^t = \frac{\exp\left(\beta_\tau^t\right)}{\sum_{l=1}^{j}\beta_l^t}, \tag{4}$$

$$h_t' = \varepsilon_t \otimes h_t = \sum_{\tau=1}^{j} \varepsilon_\tau^t h_\tau^t, \tag{5}$$

where $y = \beta_0 + \beta_1 x_1 + \beta_2 x_2 + \beta_3 x_3 + \varepsilon$ represents the matrix product, and h_t represents the hidden layer state matrix of LSTM.

Within the prediction scale of 4 h, corrected WS in NWP was used to judge the fluctuation. If the fluctuation is lower than the set threshold at some point, the STAN model is used for WPP.

2.2. Modeling of WPP Based on WSPC. The WSPC is a static curve reflecting wind power characteristics obtained by fitting a large number of historical WS and power data and does not reflect the time continuity of wind power [25, 26]. Compared with the modeling method based on artificial intelligence, it is not affected by the predictability of time series at the time points of high WS fluctuation and is suitable for wind power prediction at the time points of high WS fluctuation. The actual wind speed and power data are used for modeling, and the modified WS is used as input to obtain the predicted power. The fitting result of univariate linear regression is a straight line, which cannot reflect the actual output characteristics of the wind farm. Therefore, the polynomial regression algorithm is first used to raise the wind speed to three dimensions, and then the WSPC is fitted based on the multiple linear regression algorithm, which is used as the prediction model of high fluctuation time points. The principle of the multiple linear regression algorithm is shown in the following equation.

$$y = \beta_0 + \beta_1 x_1 + \beta_2 x_2 + \beta_3 x_3 + \varepsilon, \tag{6}$$

where β_0 is a constant term, $\beta_0 \sim \beta_3$ represents the partial regression coefficient, which represents the average change in y when $x_i\,(i = 1, 2, 3)$ increasing or decreasing by one unit with the other independent variables held constant, and ε is the random error.

2.3. The Dynamic Switching Mechanism of Multiple WPP Models. In this paper, wind speed fluctuation is described by the change rate of wind speed, and the threshold of wind speed fluctuation is set. Since the chaos degree of time series with severe fluctuations will increase, the predictability of the neural network model will decrease [27]. The schematic diagram of the switching mechanism is shown in Figure 1. The USTWPP model provides the prediction power sequence for the next 4 h, and the length is 16. The STAN model is used for prediction when the wind speed fluctuation is lower than the threshold, the WSPC model is used for prediction when the WS fluctuation is higher than the threshold, and then the prediction sequence is reconstructed in time order.

When the WSPC is used to predict at a certain point, the measured WS cannot be obtained, so it is necessary to correct the WS of NWP to improve the prediction accuracy. In this paper, the WS correction model proposed in the literature [28] is adopted, and the LSTM is used for modeling. The WS correction strategy is shown in Figure 2.

The WS correction is performed in a multitask learning manner, i.e., the corrected WS for the next 4 h is output directly at a prediction time. The input of the model is the Historical WS (His WS) and the forecast WS 4 h before the start time, including 30 m WS, 100 m WS, and their average WS (AVE WS).

For the time point of high fluctuation of wind speed, the prediction model was switched to the WSPC model to complete the prediction model switching.

2.4. The Model Evaluation Index of WPP. In this paper, three metrics, normalized root mean square error (NRMSE), normalized mean absolute error (NMAE), and correlation coefficient (I) are used to evaluate the performance of the proposed ultrashort-term wind power prediction model. The NRMSE is calculated as shown in the following equation.

$$\mathrm{NRMSE} = \sqrt{\frac{\sum_{i=1}^{n}\left(y_i - \widehat{y}_i\right)^2}{nCap^2}}, \tag{7}$$

where y_i represents the actual power at the moment i, $\widehat{y}_i$ represents the predicted power at the moment i, n represents the length of the test set, and Cap represents the installed capacity of the WF.

The NMAE is calculated as shown in the following equation.

$$\mathrm{NMAE} = \frac{1}{n}\sum_{i=1}^{n}\frac{\left|y_i - \widehat{y}_i\right| \times 100\%}{Cap}. \tag{8}$$

The correlation coefficient is calculated as shown in the following equation.

$$I = \frac{\mathrm{cov}\left(y, \widehat{y}\right)}{\sqrt{D(y) \times D\left(\widehat{y}\right)}}, \tag{9}$$

where $\mathrm{cov}(\cdot)$ represents the covariance and $D(\cdot)$ represents the variance.

3. The Technology Route of WPP

The technical route of the WPP model is shown in Figure 3 and consists of the following steps:

(1) Divide the data into training sets and test sets, and fit the WSPC on the training set according to equation (6)

(2) Construct the spatiotemporal attention neural network (STAN), train the STAN model training set, and obtain the USTWPP model

(3) In the prediction stage, the LSTM model is used as a modifier. The forecasting wind speed in NWP for the next 4 hours is revised

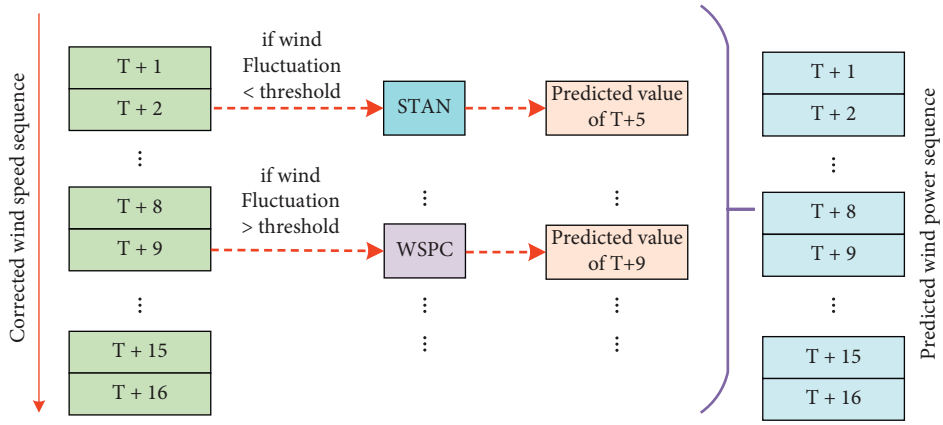

Figure 1: The schematic diagram of the switching mechanism.

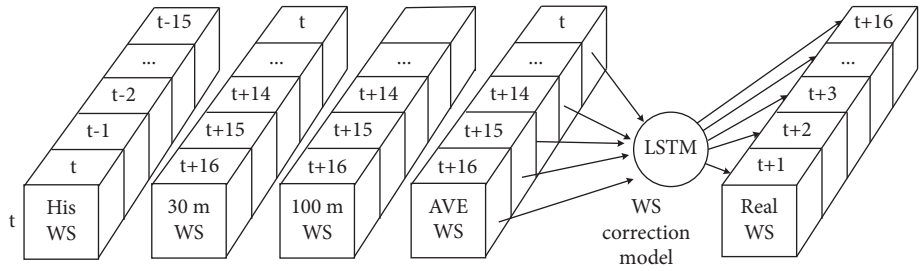

Figure 2: Wind speed correction strategy.

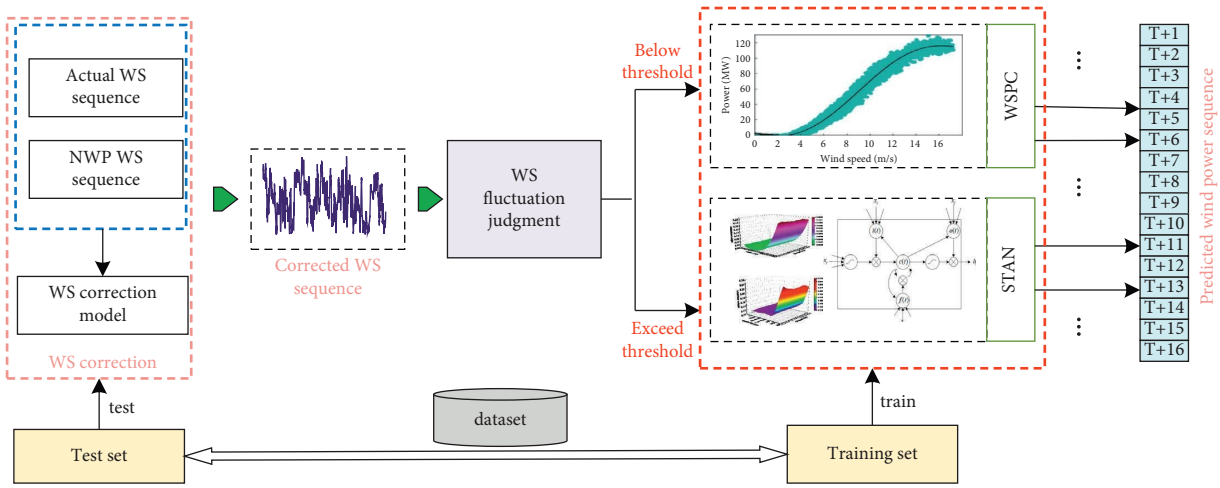

Figure 3: Technology roadmap.

(4) The WS fluctuation in the next 4 hours is judged on the modified WS sequence. If the WS fluctuation exceeds the threshold at a certain time, the WSPC model is used to predict the moment. If the WS fluctuation at a certain time is lower than the threshold, the STAN model is used to predict

(5) If the modified WS at a certain time is lower than the cut-in WS of the wind turbine, the predicted result at that time is set to 0. Reconstruct the prediction results in chronological order.

4. Example Analysis

The data provided by a WF with an installed capacity of 130.5 MW is used for experimental validation, and the cut-in WS of the turbine is 3.5 m/s. The data span from March 1, 2020, 0 : 00, to September 7, 2020, 23 : 30, includes actual wind speed data, actual power data, and NWP, and the data resolution is 15 min. The samples of the last 30 days are taken as the test set, and the remaining samples are the training set. The input features include WS, WD, temperature (T), humidity (Hum), and air pressure (AP), where the WD is sine

and cosine processed as statistical features. The modeling input step is 16 and the output step is also 16, i.e., 16 steps of ultrashort-term multistep prediction are performed. The model adopts a multitask learning mode, i.e., the predicted power of 16 points is output at one time instead of rolling iterative prediction, which can avoid the impact of error accumulation to a certain extent.

The LSTM layer of the network structure contains 16 neurons, the depth of the network is 3, the computer CPU parameters are Intel (R) Core (TM) i5-7300HQ CPU @ 2.50 GHz, the memory is 16 GB, and the training parameters are as follows: where a total of 100 epochs are trained, bach_size is set to 128, to mitigate overfitting, drop_out is set to 0.2, and the learning_rate is set to 0.1. To reduce the complexity of the model, an early stopping strategy is used, and the model stops training when the actual iteration reaches the 11th epoch. The model is trained for a total of 128 m, and the prediction time for each sample is 0.02 ms, which meets the business requirement of USTWPP.

The WSPC is shown in Figure 4, and the fitted curve is distributed in the middle of the scatter, which can effectively represent the wind power output characteristics, and the model is used for the prediction of high wind speed fluctuation samples.

The attention distribution of the spatiotemporal attention neural network is shown in Figure 5. As shown in Figure 5(a), the highest spatial feature contribution is the historical power, followed by the wind speed. Because it is the wind speed attribute in NWP, it is not clearly reflected with the wind power, so the feature contribution is lower than the historical power. The attention weight of the other features is lower, and the direct correlation with wind power is weak. Combined with Figure 5(b), we can discover that the temporal attention weight shows a monotonically increasing trend in steps 3–16. It is because the time series does not change dramatically over the 1–4 hour prediction scale, the autocorrelation of time series plays an important role in ensuring the prediction accuracy. Therefore, the closer the input step length prediction domain is, the greater the time sequence feature contribution is. Because 1-2 steps are far away from the prediction domain, and its contribution to modeling evaluation is unstable, so there is an element of falsely high attention weight.

The model proposed in this paper is a kind of hybrid model (HM); it is named HM in the experimental part. The prediction curve of HM is shown in Figure 6. The prediction curve can track the actual power trajectory well, and the trend of rise and fall can be accurately captured. The crest can be accurately tracked and the low power period can be well-fitted. It indicates that HM is suitable for the USTWPP business of this wind farm.

The performance of the HM is shown in Table 1. The NRMSE of its single-step prediction is 0.054, which corresponds to an accuracy rate of 94.46%, and the prediction curve and the actual curve are strongly correlated. The prediction error gradually increases with the increase of the prediction step. For the future 16th step, the NRMSE is 0.0907, which corresponds to an accuracy of 90.93%, i.e., the

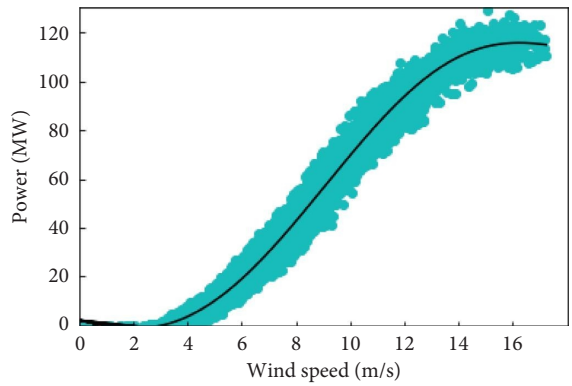

Figure 4: Wind speed-power curve.

average error is less than 10% of the installed capacity, thus proving the applicability of the HM.

The prediction curves of the 2412th sample in the test set are shown in Figure 7(a), and the corresponding WS curve is shown in Figure 7(b). Based on the prediction results of the STAN model, the corrected wind speeds of the 1st–5th prediction time points are all lower than 3.5 m/s, so their prediction results are replaced by 0. The error of the corrected power values is lower, and HM can effectively correct the power prediction errors in extremely low output cases.

The prediction curve of the 313th sample of the test set is shown in Figure 8(a), and the corresponding WS curve is shown in Figure 8(b). The switching of the prediction result in the 3rd step of the STAN model is caused by the large fluctuation value of the WS correction result in the 3rd step, and the prediction result after the switching is closer to the actual power, so this switching is effective.

For sample 2819, the switching mechanism works inversely and its prediction curve is shown in Figure 9(a), and the corresponding WS curve is shown in Figure 9(b). The WS fluctuations at steps 11 and 14 lead to a switch in the prediction model at the corresponding time point of the STAN model. However, the prediction curve after the switch deviates from the actual power curve to a greater extent, and this type of switch is called a harmful switch. In the test set of 2880 samples, 435 times of switching occurred, among which 38 times of unfavorable switching accounted for 8.74%. Harmful switching is mainly caused by incorrect wind speed correction, and abnormal data caused by wind power restrictions in wind farms will also cause harmful switching.

The performance of the HM model was compared with the LSTM model, bidirectional long and short-term memory neural network (BiLSTM) model, extreme learning machine (ELM) model, and Random Forest (RF) model. The NRMSE, NMAE, and I are used to evaluate the performance of the 16th step prediction, the comparison results are shown in Table 2, and HM and RF model obtain the lowest and highest NRMSE, respectively. Overall, the recurrent neural network has a stronger performance for USTWPP, and the machine learning model has a slightly worse performance. BiLSTM is a combination of forward LSTM and backward LSTM, which can extract time sequence information in both

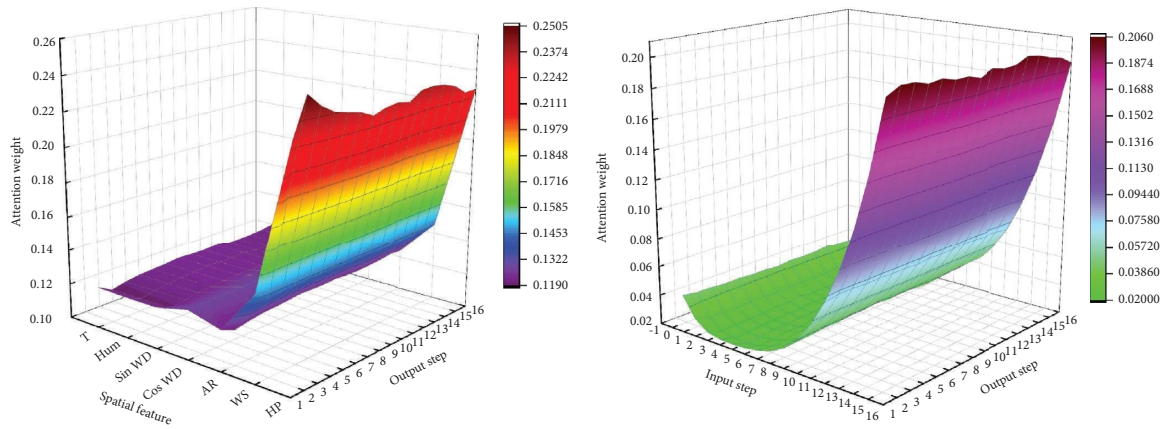

Figure 5: Attention weight distribution: (a) spatial attention weight distribution and (b) temporal attention weight distribution.

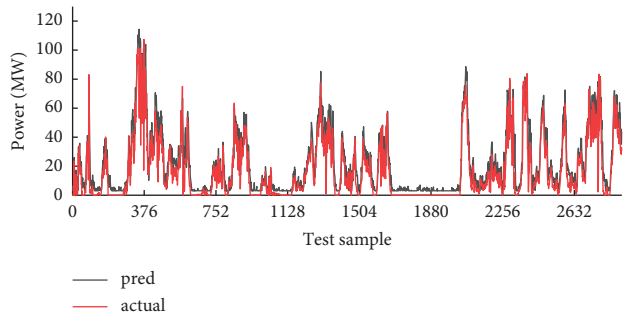

Figure 6: The 16th step prediction curve of HM.

Table 1: Predicted performance of HM.

Predicted_step	NRMSE	NMAE	I
1	0.0540	0.0510	0.9354
4	0.0636	0.0515	0.8514
8	0.0740	0.0634	0.7591
12	0.0824	0.0696	0.6898
16	0.0907	0.0756	0.6025

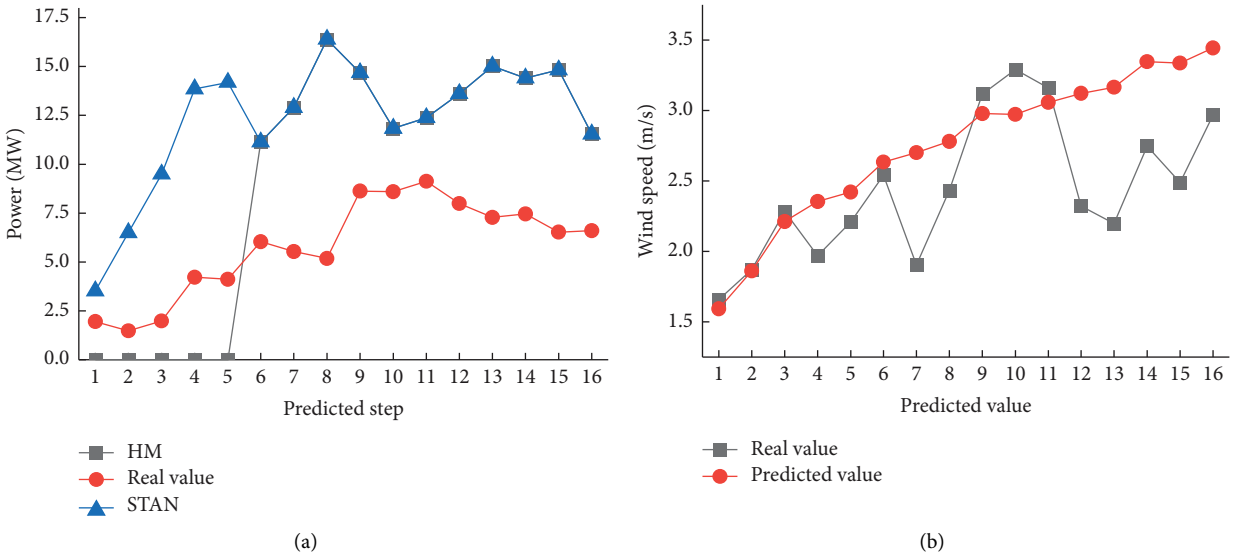

Figure 7: Applicability analysis of HM model for extremely low output scenarios: (a) power prediction curve and (b) wind speed correction curve.

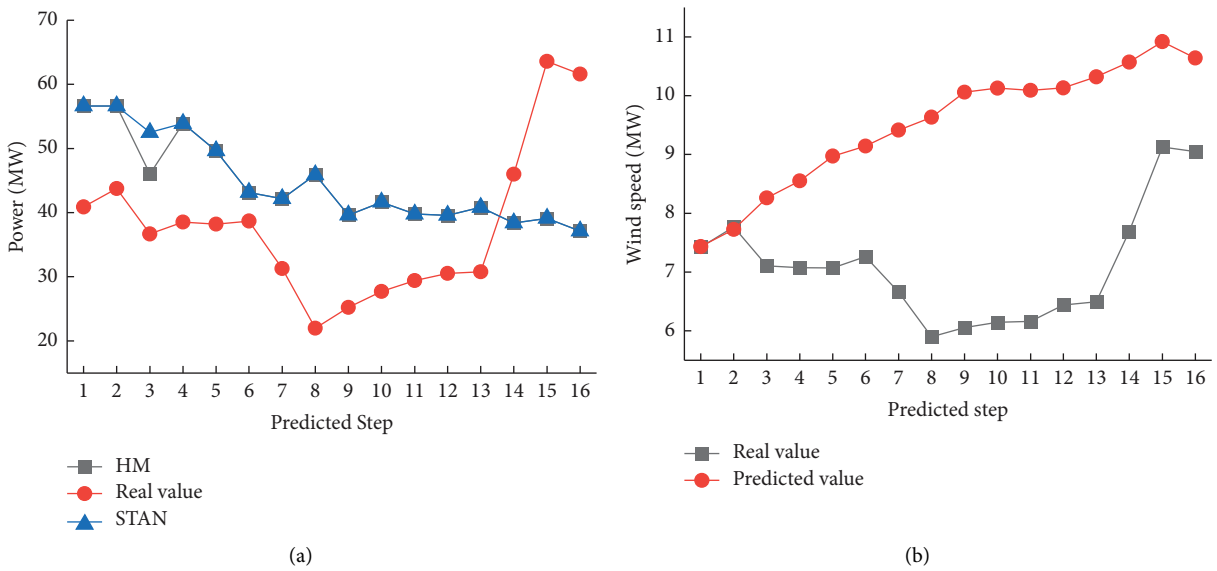

Figure 8: Applicability analysis of HM model for high WS fluctuation scenarios: (a) power prediction curve and (b) wind speed correction curve.

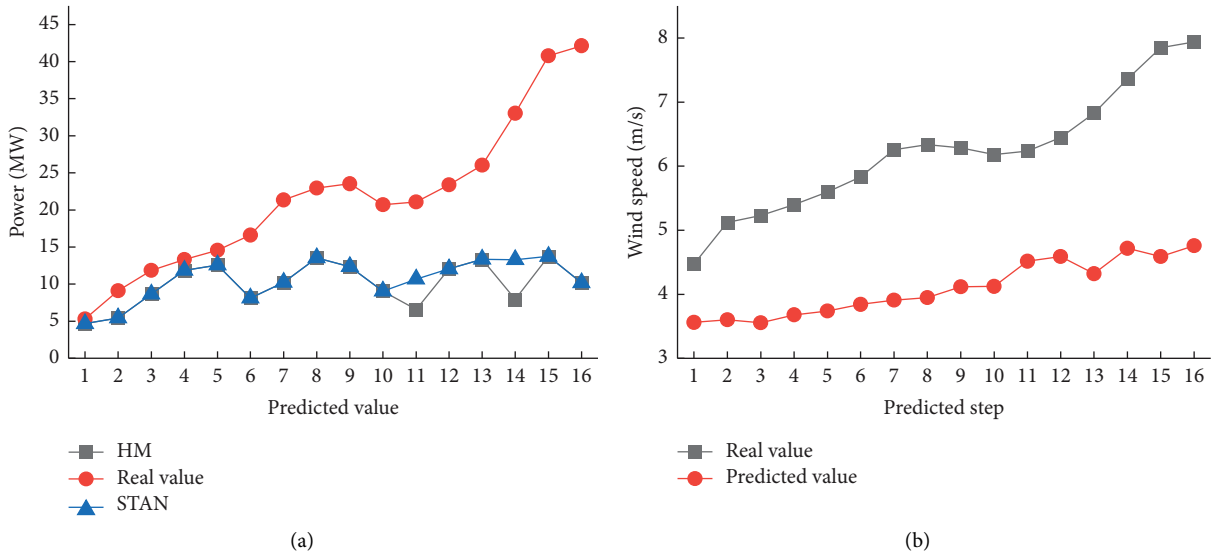

Figure 9: Limitation analysis of the HM model when the accuracy of WS correction is insufficient: (a) power prediction curve and (b) wind speed correction curve.

Table 2: The 16th step NRMSE comparison of HM and other models.

Index	LSTM	BiLSTM	ELM	RF	HM
NRMSE	0.1031	0.1012	0.1047	0.1123	0.0907
NMAE	0.0903	0.0912	0.0943	0.0878	0.0756
I	0.5548	0.5673	0.5598	0.5423	0.6025

forward and backward directions. There is no consensus on which model is more suitable for USTWPP. In this paper, the NRMSE of the BiLSTM model is lower than the LSTM model, while the NMAE is lower than the LSTM model, and the correlation coefficient is higher than that of the LSTM model. On the whole, the performance of the BiLSTM model is better.

5. Conclusion

A multimodel dynamic switching output mechanism for an ultrashort-term WPP model is proposed, and simulation experiments are conducted on data provided by a WF with an installed capacity of 130.5 MW in China. The following conclusions are obtained:

Data Availability

The data used to support the findings of this study are available from the corresponding author upon request.

Conflicts of Interest

The authors declare that they have no conflicts of interest.

Authors' Contributions

RF and BW designed this study. XW and CH organized the database. LZ contributed to the modeling of WSPC. WT contributed to the design of STAN structure. KZ contributed to the theoretical research of switching mechanism. XH and WD constructed the experimental environment and completed the experimental analysis. All authors contributed to the writing of the article and all agreed to the submitted version of the article.

Acknowledgments

This work was supported by the NARI Group Science and Technology Project (524609220153).

References

[1] N. Safari, C. Y. Chung, and G. C. D. Price, "Novel multi-stepshort-term wind power prediction framework based on chaotic time series analysis and singular spectrum analysis," *IEEE Transactions on Power Systems*, vol. 33, no. 1, pp. 590–601, 2018.

[2] C. Zhao, C. Wan, and Y. Song, "Operating reserve quantification using prediction intervals of wind power: an integrated probabilistic forecasting and decision methodology," *IEEE Transactions on Power Systems*, vol. 36, no. 4, pp. 3701–3714, 2021.

[3] Z. Li, X. Luo, M. Liu, X. Cao, S. Du, and H. Sun, "Wind power prediction based on EEMD-Tent-SSA-LS-SVM," *Energy Reports*, vol. 8, no. 8, pp. 3234–3243, 2022.

[4] Y. Sun, Y. Huang, and M. Yang, "Ultra-short-term wind power interval prediction based on fluctuating process partitioning and quantile regression forest," *Frontiers in Energy Research*, vol. 317, 2022.

[5] Y. Li, B. Wang, Z. Yang, J. Li, and G. Li, "Optimal scheduling of integrated demand response-enabledcommunity-integrated energy systems in uncertain environments," *IEEE Transactions on Industry Applications*, vol. 58, no. 2, pp. 2640–2651, 2022.

[6] Y. Li, R. Wang, Y. Li, M. Zhang, and C. Long, "Wind power forecasting considering data privacy protection: a federated deep reinforcement learning approach," *Applied Energy*, vol. 329, Article ID 120291, 2023.

[7] M. B. Ozkan and P. Karagoz, "Reducing the cost of wind resource assessment: using a regional wind power forecasting method for assessment," *International Journal of Energy Research*, vol. 45, no. 9, Article ID 13182, 2021.

[8] Q. Xue and Y. Z. Z. Collaborative, "Optimization of sustainable energy systems and PV-greenhouses in rural areas," *IEEE Transactions on Sustainable Energy*, vol. 14, no. 1, pp. 642–656, 2023.

[9] X. Fu, Q. Guo, and H. Sun, "Statistical machine learning model for stochastic optimal planning of distribution networks considering a dynamic correlation and dimension reduction," *IEEE Transactions on Smart Grid*, vol. 11, no. 4, pp. 2904–2917, 2020.

[10] M. A. Al-qaness, A. A. Ewees, H. Fan, L. Abualigah, and M. A. Elaziz, "Boosted ANFIS model using augmented marine predator algorithm with mutation operators for wind power forecasting," *Applied Energy*, vol. 314, Article ID 118851, 2022.

[11] S. Khazaei, M. Ehsan, and S. Soleyman, "A high-accuracy hybrid method for short-term wind power forecasting," *Energy*, vol. 238, 2022.

[12] C. Yildiz, H. Acikgoz, D. Korkmaz, and U. Budak, "An improved residual-based convolutional neural network for very short-term wind power forecasting," *Energy Conversion and Management*, vol. 228, no. 1, Article ID 113731, 2021.

[13] N. Huang, Y. Wu, G. Lu, W. Wang, and X. Cao, "Combined probability prediction of wind power considering the conflict of evaluation indicators," *IEEE Access*, vol. 7, no. 7, Article ID 174709, 2019.

[14] I. Gonzalez-Aparicio, F. Monforti, P. Volker et al., "Simulating European wind power generation applying statistical downscaling to reanalysis data," *Applied Energy*, vol. 199, pp. 155–168, 2017.

[15] F. Shahid, A. Zameer, A. Mehmood, and M. A. Z. Raja, "A novel wavenets long short term memory paradigm for wind power prediction," *Applied Energy*, vol. 269, Article ID 115098, 2020.

[16] Z. Lin, X. Liu, and M. Collu, "Wind power prediction based on high-frequency SCADA data along with isolation forest and deep learning neural networks," *International Journal of Electrical Power & Energy Systems*, vol. 118, Article ID 105835, 2020.

[17] B. Khorramdel, C. Y. Chung, N. Safari, and G. C. D. Price, "A fuzzy adaptive probabilistic wind power prediction framework using diffusion kernel density estimators," *IEEE Transactions on Power Systems*, vol. 33, no. 6, pp. 7109–7121, 2018.

[18] F. Shahid, A. Zameer, and M. Muneeb, "A novel genetic LSTM model for wind power forecast," *Energy*, vol. 223, Article ID 120069, 2021.

[19] H. Wang, S. Han, Y. Liu, J. Yan, and L. Li, "Sequence transfer correction algorithm for numerical weather prediction wind speed and its application in a wind power forecasting system," *Applied Energy*, vol. 237, pp. 1–10, 2019.

[20] R. Yu, Z. Liu, X. Li et al., "Scene learning: deep convolutional networks for wind power prediction by embedding turbines into grid space," *Applied Energy*, vol. 238, pp. 249–257, 2019.

[21] O. Abedinia, M. Lotfi, M. Bagheri, B. Sobhani, M. Shafie-khah, and J. P. S. Catalao, "Improved EMD-based complex prediction model for wind power forecasting," *IEEE Transactions on Sustainable Energy*, vol. 11, no. 4, pp. 2790–2802, 2020.

[22] C. Li, G. Tang, X. Xue, X. Chen, R. Wang, and C. Zhang, "The short-term interval prediction of wind power using the deep learning model with gradient descend optimization," *Renewable Energy*, vol. 155, pp. 197–211, 2020.

[23] Z. Xing, B. Qu, Y. Liu, and Z. Chen, "Comparative study of reformed neural network based short-term wind power forecasting models," *IET Renewable Power Generation*, vol. 16, no. 5, pp. 885–899, 2022.

[24] X. Fu, "Statistical machine learning model for capacitor planning considering uncertainties in photovoltaic power," *Protection and Control of Modern Power Systems*, vol. 1, pp. 51–63, 2022.

[25] Q. Chen and K. A. Folly, "Short-term wind power forecasting using mixed input feature-basedcascade-connected artificial

neural networks," *Frontiers in Energy Research*, vol. 9, pp. 1–12, 2021.

[26] L. Kou, Y. Li, F. Zhang et al., "Review on monitoring, operation and maintenance of smart offshore wind farms," *Sensors*, vol. 22, no. 8, p. 2822, 2022.

[27] C. Liu, X. Zhang, S. Mei et al., "Numerical weather prediction enhanced wind power forecasting: rank ensemble and probabilistic fluctuation awareness," *Applied Energy*, vol. 313, Article ID 118769, 2022.

[28] Z. M. Hamza, K. N. Mujeeb, M. Mansoor, F. M. Adeel, K. R. M. Syed, and S. Filippo, "Adaptive ML-based technique for renewable energy system power forecasting in hybrid PV-Wind farms power conversion systems," *Energy Conversion and Management*, vol. 258, 2022.